Identification of the 0^+ proton pairing vibration state in the doubly magic nucleus ^{208}Pb by particle spectroscopy

A. Heusler,[1,*] T. Faestermann,[2] R. Hertenberger,[3] H.-F. Wirth,[2,3] and P. von Brentano[4]

[1]*Gustav-Kirchhoff-Strasse 7/1, D-69120 Heidelberg, Germany*

[2]*Physik Department E12, Technische Universität München, D-85748 Garching, Germany*

[3]*Department für Physik, Ludwig-Maximilian-Universität München, D-85748 Garching, Germany*

[4]*Institut für Kernphysik, Universität zu Köln, D-50937 Köln, Germany*

(Received 24 November 2014; revised manuscript received 9 February 2015; published 29 April 2015)

Among about 150 levels below $E_x = 5.86$ MeV in ^{208}Pb listed by the Nuclear Data Sheets as of 2007, most levels were recently identified as particle-hole states. All natural parity states excited by the ^{208}Pb(α,α') reaction are identified, two of them are newly identified. The state at $E_x = 5667$ keV is identified as the 0^+ proton pairing vibration state. Based on the analysis of data from the ^{206,207,208}Pb(d,p), ^{208}Pb(d,d'), and ^{208}Pb(p,p') reactions obtained with the Q3D magnetic spectrograph of the Maier-Leibnitz-Laboratorium at Garching (Germany) at scattering angles $15^\circ \leqslant \Theta \leqslant 138^\circ$ and bombarding energies $E_d = 22,24$ MeV and $14.8 < E_p < 18.2$ MeV, the excitation energy is determined as $E_x = 5666.7 \pm 0.3$ keV; the mean cross section in the nonresonant ^{208}Pb(p,p') and the ^{208}Pb(d,d') reactions is about 1 μb/sr. A new state at $E_x = 5042 \pm 3$ keV is suggested to have the spin of 2^+. The 0^+ neutron pairing vibration state at $E_x = 4868$ keV and the 0^+ member of the double-octupole multiplet at $E_x = 5241$ keV are verified by the nonresonant ^{208}Pb(p,p') and ^{208}Pb(d,d') reactions with cross sections of around 3 μb/sr.

DOI: 10.1103/PhysRevC.91.044325 PACS number(s): 21.10.−k, 21.30.Fe, 27.80.+w

I. INTRODUCTION

The doubly magic nucleus ^{208}Pb is a fascinating object to study nuclear forces. Among more than 300 known levels [1], most bound states are described by the shell model [2–4] with one-particle one-hole configurations [1,5–16].

Yet at rather low excitation energies multi-particle-hole states show up. The double octupole (d.o.) 0^+ state is identified at $E_x = 5241$ keV [17,18], only 12 keV above the predicted energy of twice the energy of the 3^- yrast state. The neutron pairing vibration state is identified at 4868 keV [19,20], close to the predicted energy [21–24]. The proton pairing vibration state, however, is not yet known.

We identify the proton pairing vibration state at $E_x = 5666.7 \pm 0.3$ keV based on the clear excitation by the ^{208}Pb(α,α') reaction [25–28] and the agreement of the excitation energy with the prediction by Blomqvist *et al.* [21,22]. The 0^+ neutron pairing vibration state at $E_x = 4868$ keV and the 0^+ member of the d.o. multiplet at $E_x = 5241$ keV are verified by particle spectroscopy.

Prerequisites are the good precision and the high sensitivity of the Q3D magnetic spectrograph at the Maier-Leibnitz-Laboratorium (MLL Garching, Germany) [29,30] which allowed to identify most states below 8 MeV in ^{208}Pb with cross sections varying from less than 1 to nearly 1000 μb/sr [5–15]. Excitation energies are determined with uncertainties of typically 0.5 keV, but down to 10 eV for isolated and strongly excited states.

II. MOTIVATION

A. Nuclear shell model

The shell model in its simplest form assuming the surface δ interaction [4] describes the excitation energies of the particle-hole states in the doubly magic nucleus ^{208}Pb by one parameter which is derived from the multiplet splitting in ^{210}Po. The relative excitation energies in the ground state (g.s.) multiplet of ^{210}Po are reproduced within 2% [4,6,11]. The lowering of the 0^+ state in the g.s. multiplet of a dozen neighbors of the known doubly magic nuclei heavier than ^{50}Ti is also explained within about 5% [6].

The interaction between the particle LJ and the hole lj in the particle-hole configurations $LJ\,lj$ is reigned by the classical angle between their orbits [31] in four classes defined by two geometrical coefficients depending on the nature of parity

$$U_p(L,l,I) = (-1)^{L+l+I} \tag{1}$$

and the Nordheim number [3]

$$N_h(LJ,lj) = (-1)^{L+l+J+j-1}. \tag{2}$$

Here I is the spin of the particle-hole configuration $LJ\,lj$, L,l are the angular momenta and J,j are the spins of the particle and the hole, respectively. Because of the double magicity, the level density in ^{208}Pb is low. Below $E_x = 3.9$ MeV, there are only five states and at $3.9 \leqslant E_x \lesssim 5.8$ MeV about 110 states are identified with certainty [1,5–15].

At $E_x < 5.8$ MeV, the range of spins is from 1^+ to 11^+ and from 0^- to 8^-. The mean number of states with the same spin and parity is between one and six by excepting the 11, 13, and 12 states with spins 3^-, 4^-, and 5^-. Nevertheless because of the multitude of spins and the two parities, about one-third of the states have spacings less than 3 keV.

*Corresponding author: A.Heusler@mpi-hd.mpg.de

We define an energy label $\tilde{E}_x$ for each state by taking the excitation energy rounded to full keV but varied within ± 2 keV in order to obtain uniqueness. The final resolution obtained with particle spectroscopy is limited to about 3 keV because of the unavoidable atomic electrons (Sec. III C 1). Indeed, a resolution of 1.5 keV half-width at half-maximum on the low energy side is obtained with the Q3D magnetic spectrograph at the MLL (Garching, Germany) [8].

B. Natural parity states

The schematic shell model without residual interaction (SSM) [8] describes many states in ^{208}Pb by one-particle one-hole configurations. The energies E_x^{SSM} are determined by the masses of the nuclei ^{207}Tl, ^{209}Bi, ^{207,208,209}Pb and assumed Coulomb displacement energies

$$\begin{aligned} \delta E_{\mathrm{Coul}}^{\nu,SSM}(\mathrm{ph}) &= 0.0\ \mathrm{MeV} \quad \text{for neutrons and} \\ \delta E_{\mathrm{Coul}}^{\pi,SSM}(\mathrm{ph}) &= -0.3\ \mathrm{MeV} \quad \text{for protons.} \end{aligned} \tag{3}$$

At $E_x^{SSM} < 5.843$ MeV in ^{208}Pb, the SSM predicts 60 negative parity particle-hole states and 34 positive parity particle-hole states, hence 47 states with natural parity $U_p = +1$ [Eq. (1)].

Essentially, the ^{208}Pb(α,α') reaction does not excite states with unnatural parity but only natural parity states. As Table I shows, about 40 levels are observed at $E_x < 5.8$ MeV with certainty by Atzrott [25] and Valnion *et al.* [27,28] and a dozen levels with upper limits 20 μb/sr of the cross section at $\Theta = 25^\circ$ [27,28] while 47 natural parity states are expected by the SSM.

The nonresonant ^{208}Pb(p,p') reaction excites natural parity states with similar strengths as the ^{208}Pb(α,α') reaction. The strengths β_L shown in Table I mostly agree for both reactions. However, the ^{208}Pb(p,p') [and ^{208}Pb(d,d')] reaction excites also unnatural parity states with similar cross sections.

C. Multi-particle-hole states

Below $E_x = 6$ MeV, at least six states are expected which are not described by one-particle one-hole configurations; at higher excitation energies even more multi-particle-hole states are expected [23,24].

1. Identification of double octupole states

The d.o. multiplet with spins $0^+, 2^+, 4^+, 6^+$ is predicted at twice the energy of the 3^- yrast state [1],

$$\begin{aligned} E_x(3_1^-) &= 2614.522 \pm 0.010\ \mathrm{keV}, \\ E_x(d.o.) &= 2E_x(3_1^-) = 5229\ \mathrm{keV}. \end{aligned} \tag{4}$$

Indeed the 0^+ member is identified at $E_x = 5241$ keV by the ^{208}Pb$(n,n'\gamma)$ reaction [17]; its dominant structure as d.o. configuration was shown by the γ transition to the 3^- yrast state [18]. The existence of the state was proven by the ^{208}Pb(p,p') reaction with $E_p = 22$ MeV and the ^{208}Pb(α,α') reaction with $E_\alpha = 40$ MeV [27,28].

Two other members of the d.o. multiplet are identified, as well: the 5286 state as the 2^+ member and the 5216 state as the 4^+ member [18]. The 6^+ member is mixed with the large number of particle-hole configurations; most of them but not all are identified [8].

2. Identification of the neutron pairing vibration state

The excitation energy of the neutron pairing vibration 0^+ state in ^{208}Pb is predicted [21,22] from the ground state binding energies of the neighboring nuclei [32] as

$$\begin{aligned} E_x(0_\nu^+) &= [m(^{210}\mathrm{Pb}) + m(^{206}\mathrm{Pb}) - 2m(^{208}\mathrm{Pb})]c^2 \\ &\quad + 4\delta E_{\mathrm{Coul}}^{\nu}(\mathrm{ph}), \\ &= 4980\ \mathrm{keV} + 4\delta E_{\mathrm{Coul}}^{\nu}(\mathrm{ph}), \end{aligned} \tag{5}$$

where c is the speed of light. The Coulomb displacement energy $\delta E_{\mathrm{Coul}}^{\nu}(\mathrm{ph})$ results from the monopole particle-hole interaction energy between the 0^+ particle pair in ^{210}Pb and the 0^+ hole pair in ^{206}Pb [21].

The neutron pairing vibration 0^+ state was identified by the two-neutron transfer reactions ^{206}Pb(p,t) and ^{210}Pb(t,p) [19,20]; the spin of 0^+ was first determined by Bjerregaard *et al.* [33] in the ^{206}Pb(t,p) reaction. The ^{208}Pb$(n,n'\gamma)$ reaction yielded a more precise excitation energy [1,17].

3. Prediction of the proton pairing vibration state

Similar to the neutron pairing vibration state [Eq. (5)], the excitation energy for the proton pairing vibration state is predicted [21] as

$$\begin{aligned} E_x(0_\pi^+) &= [m(^{210}\mathrm{Po}) + m(^{206}\mathrm{Hg}) - 2m(^{208}\mathrm{Pb})]c^2 \\ &\quad + 4\delta E_{\mathrm{Coul}}^{\pi}(\mathrm{ph}), \\ &= 6600\ \mathrm{keV} + 4\delta E_{\mathrm{Coul}}^{\pi}(\mathrm{ph}), \end{aligned} \tag{6}$$

The masses are known within better than 1.5 keV except for ^{206}Hg where the uncertainty is 20 keV [32].

Together with the value of the Coulomb displacement energy obtained for all configurations at $E_x^{SSM} < 6361$ keV [Eq. (9)] determined in the following section (Sec. II D), the proton pairing vibration 0^+ state is expected at

$$5.4 \lesssim E_x \lesssim 5.9\ \mathrm{MeV}. \tag{7}$$

By this work, the 5667 state [26–28] is identified as the proton pairing vibration 0^+ state (Sec. IV B, Figs. 1, 2, and Tables I, III, IV).

D. The Coulomb displacement energy

The Coulomb displacement energies $\delta E_{\mathrm{Coul}}^{\nu}(\mathrm{ph})$ and $\delta E_{\mathrm{Coul}}^{\pi}(\mathrm{ph})$ can be obtained from the difference between the SSM energies [8] and the centroids of the particle-hole multiplets in ^{208}Pb [12]. For neutrons the lowest configurations

TABLE I. Levels at $4.5 < E_x < 6.1$ MeV observed by the ^{208}Pb(α,α') reaction. Below $E_x = 4.5$ MeV ten more states (all with natural parity) are observed [1,25–28]. The proton pairing vibration state is identified as $\tilde{E}_x = 5667$ (Sec. IV B); the 5042 state is newly identified (both printed bold face).

	I^π_m	Nuclear Data Sheets	^{208}Pb(α,α')				^{208}Pb(p,p')
	[12]	[1]	[27,28]		[25]		[34]
$\tilde{E}_x$	[a]	E_x keV	E_x keV	$\sigma(25^\circ)$ μb/sr	E_x keV	β_L [b] $\times 10^4$	β_L [b] $\times 10^3$
4611	8^+_1	4610.748 $\pm$ 0.016	4610.7 $\pm$ 0.8	144	4610.2 $\pm$ 0.3	267	40
4698	3^-_4	4698.323 $\pm$ 0.017	4698.3 $\pm$ 0.8	242	4698.3 $\pm$ 0.5	377[c]	33
4710	5^-_7	4708.727 $\pm$ 0.021	4715 $\pm$ 5	30	[c]		[d]
4842	1^-_1	4841.60 $\pm$ 0.05	4841.3 $\pm$ 0.8	224	4840.8 $\pm$ 1.7	[d]	[d]
4861	8^+_2	4860.78 $\pm$ 0.06	4856 $\pm$ 3	20	4864.4 $\pm$ 1.4	[d]	[d]
4895	10^+_1	4895.23 $\pm$ 0.05	4895.0 $\pm$ 0.8	< 20	4895.0 $\pm$ 0.5	108	27
4937	3^-_5	4937.19 $\pm$ 0.04	4937.0 $\pm$ 0.8	25	4938.6 $\pm$ 0.1	153	(24, $L = 4$)
4974	3^-_6	4973.918 $\pm$ 0.019	4974.0 $\pm$ 0.8	156	4974.5 $\pm$ 0.5	226	26
5042	2^+ [e]	[d]	5038.1 $\pm$ 0.8	34	5038.6 $\pm$ 0.1	[d]	[d]
5069	10^+_2	5069.31 $\pm$ 0.10	[c]		[c]		[d]
5075	5^-_8	5075.78 $\pm$ 0.18	5073.7 $\pm$ 1.5	48[c]	5076.1 $\pm$ 0.5	(207[c], $L = 10$)	(39, $L = 9$)
5085	7^-_3	5085.470 $\pm$ 0.024	5084.0 $\pm$ 1.5	50	5086.9 $\pm$ 1.2	(107, $L = 3$)	(33, $L = 3$)
5216	4^+_2	5213.98 $\pm$ 0.03	5215.9 $\pm$ 0.8	61	5217.6 $\pm$ 1.3	[d]	[d]
5241	0^+_3	5241.1 $\pm$ 0.3	5243.0 $\pm$ 0.8	25[c]	[c]		[d]
5245	3^-_8	5245.246 $\pm$ 0.021	[c]		5245.2 $\pm$ 0.1	196[c]	[d]
5292	1^-_2	5291.90 $\pm$ 0.12	5291.6 $\pm$ 0.8	244	5293.9 $\pm$ 0.7	[d]	[d]
5347	3^-_9	5347.270 $\pm$ 0.018	5348.0 $\pm$ 0.8	87	5350.3 $\pm$ 1.2	310	35
5482	5^-_{10}	5481.87 $\pm$ 0.03	5482.8 $\pm$ 1.5	367	5487.4 $\pm$ 1.7	382[c]	45
5512	1^-_3	5511.784 $\pm$ 0.014	5512.1 $\pm$ 0.8	624[c]	[c]		(38(3)[c], $L = 1$)
5517	3^-_{11}	5516.714 $\pm$ 0.023	[c]		5516.6 $\pm$ 0.7	758[c]	(38(3)[c], $L = 3$)
5543	7^-_4	5543.01 $\pm$ 0.14	5544 $\pm$ 2	45	5543.8 $\pm$ 2.0	216	(32, $L = 3$)
5564	3^-_{12}	5563.73 $\pm$ 0.04	5563.7 $\pm$ 0.15	235	5564.4 $\pm$ 1.5	(210, $L = 2$)	(17, $L = 2$)
5640	1^-_3	5639.55 $\pm$ 0.09	5640.8 $\pm$ 0.8	27	5645.2 $\pm$ 1.2	[c]	[d]
5648	3^-_{13}	5649.01 $\pm$ 0.06	[d]		[c]		[d]
5659	5^-_{12}	5658.51 $\pm$ 0.04	5656.5 $\pm$ 1.5	25	5661.5 $\pm$ 1.2	172[c]	22
5667	$\mathbf{0^+_4}$	5665.7 $\pm$ 1.1	5665.0 $\pm$ 1.5	35	[c]		[d]
5690	4^+_4	5690.117 $\pm$ 0.023	5690.8 $\pm$ 0.8	114	5694.2 $\pm$ 1.2	363[c]	45
5716	2^+_5	5715.53 $\pm$ 0.09	5718 .4 $\pm$ 0.8	67[c]	[c]		[d]
5721	8^+_5	5721.51 $\pm$ 0.04	[c]		5722.1 $\pm$ 0.4	(184, $L = 7$)	(27, $L = 7$)
5813	3^-_{14}	5813.27 $\pm$ 0.04	5814 .5 $\pm$ 0.8	306	5816.4 $\pm$ 1.2	277[c]	28
5825	8^+_6 [f]	5825.3 $\pm$ 0.5	5835 $\pm$ 2	35	[c]		[d]
5874	3^-_{15}	5873.573 $\pm$ 0.023	5872 .1 $\pm$ 1.5	43	5873.9 $\pm$ 1.8	139	15
5996	6^+_7	5996 $\pm$ 5	5995 .4 $\pm$ 1.5	115	5994.4 $\pm$ 1.5	297	49
6010	3^-_{16}	6009.75 $\pm$ 0.04	6010.9 $\pm$ 1.5	308	6008.5 $\pm$ 1.9	353	27

[a]The order number m is determined by [12].
[b]The L-value is given if there is a mismatch with the assigned spin I^π; the value is then put in parentheses.
[c]Unresolved doublet.
[d]No data.
[e]Doublet with 5038 2^-_2 [7], $E_x = 5037.536 \pm 0.018$ keV [1]. Spin and parity are suggested (Sec. II F).
[f]Newly suggested spin. The L-satellite (Sec. III C 1) of the 5813 3^-_{14} state contributes to the peak, too.

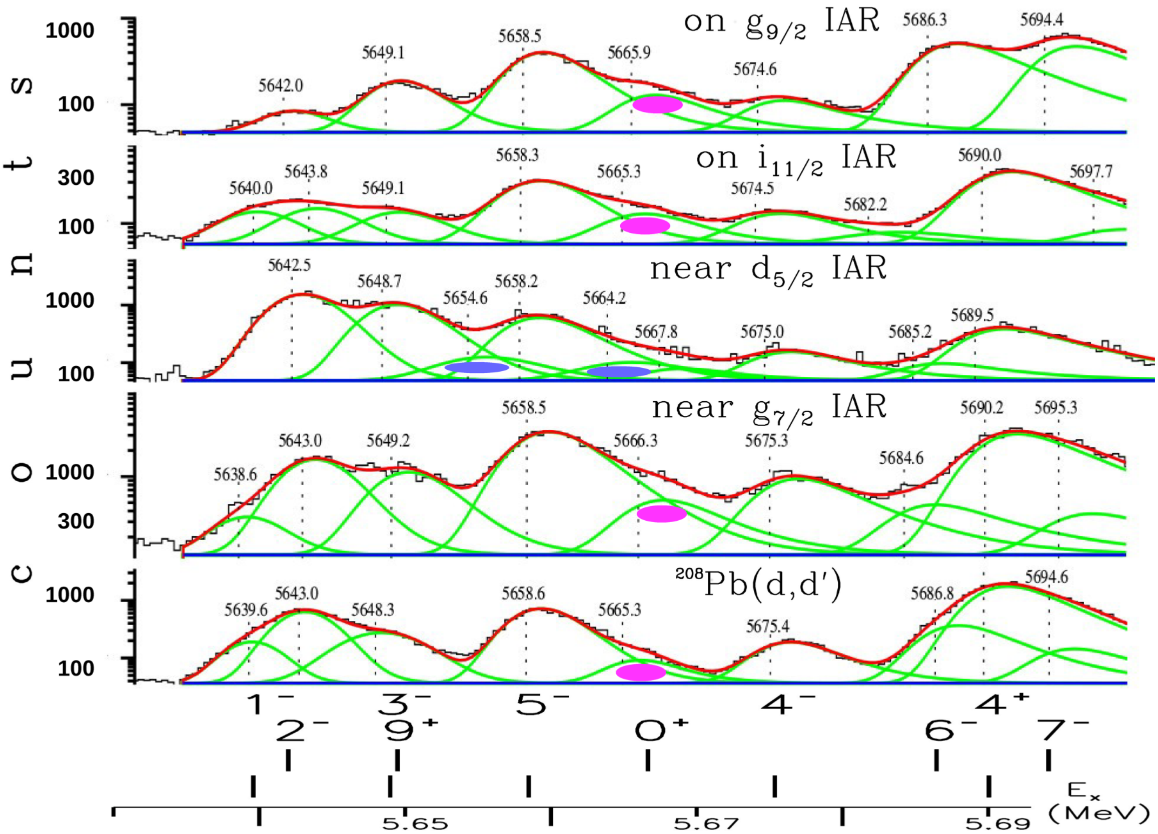

FIG. 1. (Color online) Spectra for $5.63 < E_x < 5.70$ MeV taken on the $g_{9/2}$, $i_{11/2}$, and near the $g_{7/2}$ and $d_{3/2}$ IARs and (at bottom) for ^{208}Pb(d,d'); the range of proton bombarding energies is given in Table II, the deuteron bombarding energy for (d,d') was 22 MeV. The mean distance between two peaks is 5 keV. The spectra are obtained by summing up several runs (Sec. III B). The fit by GASPAN was performed with a Gaussian followed by an exponential tail [8,39]; the dotted lines represent the center of the Gaussian. Spin and parity of all states are shown at bottom; the spins are from [8,12]. The peak from the 5667 0^+ state is marked magenta. L satellites are observed in the spectrum taken near the $j_{15/2}$ and $d_{5/2}$ IARs (marked blue). For more details see Sec. III B.

yield displacement energies

$\delta E^{\nu}_{\mathrm{Coul}}$(ph) MeV	Configuration	
−0.03	$g_{9/2}p_{1/2}$,	
−0.01	$g_{9/2}f_{5/2}$,	
+0.05	$g_{9/2}p_{3/2}$,	
−0.02	$i_{11/2}p_{1/2}$,	(8)
−0.00	$i_{11/2}f_{5/2}$,	
−0.00	$i_{11/2}p_{3/2}$,	
−0.00	$d_{5/2}p_{1/2}$,	
yielding a mean value		
-0.01 ± 0.01	for all configurations at $E_x^{SSM} \leqslant 5108$ keV.	

Individual values for protons are obtained [12] as

$\delta E^{\pi}_{\mathrm{Coul}}$(ph) MeV	Configuration	
−0.30	$h_{9/2}s_{1/2}$,	
−0.27	$h_{9/2}d_{3/2}$,	
−0.29	$h_{9/2}d_{5/2}$,	(9)
−0.08	$f_{7/2}s_{1/2}$,	
−0.24	$f_{7/2}d_{3/2}$,	
yielding a mean value		
-0.24 ± 0.06	for all configurations at $E_x^{SSM} \leqslant 6361$ keV.	

Daehnick [35] calculated the Coulomb energy with harmonic oscillator wave functions for the 12 configurations $h_{9/2}s_{1/2}$, $h_{9/2}d_{3/2}$, $h_{9/2}d_{5/2}$ with spins from 2^- to 7^-; he obtained values E_{Coul} from −0.20 to −0.24 MeV. They contain the major fraction of the displacement energy $\delta E^{\pi}_{\mathrm{Coul}}$(ph) for the proton particle-hole configurations with a $h_{9/2}$ particle [Eq. (9)]. He did not calculate the Coulomb energy for configurations with a $f_{7/2}$ particle as they are unobservable.

The displacement energies $\delta E^{\nu}_{\mathrm{Coul}}$(ph), $\delta E^{\pi}_{\mathrm{Coul}}$(ph) can be also estimated from the nonlinear increase of the Coulomb energy with the number of protons and neutrons. Bohr and Mottelson calculated them (Eq. (2-19) [36]) as

$$\delta E^{\nu}_{\mathrm{Coul}}(\mathrm{ph}) = -0.01\ \mathrm{MeV}, \tag{10}$$

$$\delta E^{\pi}_{\mathrm{Coul}}(\mathrm{ph}) = -0.18\ \mathrm{MeV}. \tag{11}$$

Curutchet *et al.* [22] estimated $\delta E^{\pi}_{\mathrm{Coul}}(\mathrm{ph}) = -0.24$ MeV.

For the neutron pairing vibration state the correction of $E_x(0^+_\nu)$ [Eq. (5)] for the Coulomb pairing force is nearly vanishing [Eqs. (8), (10)]. For the proton pairing vibration state [Eq. (6)] in contrast, the correction of $E_x(0^+_\pi)$ is large [Eqs. (9), (11)].

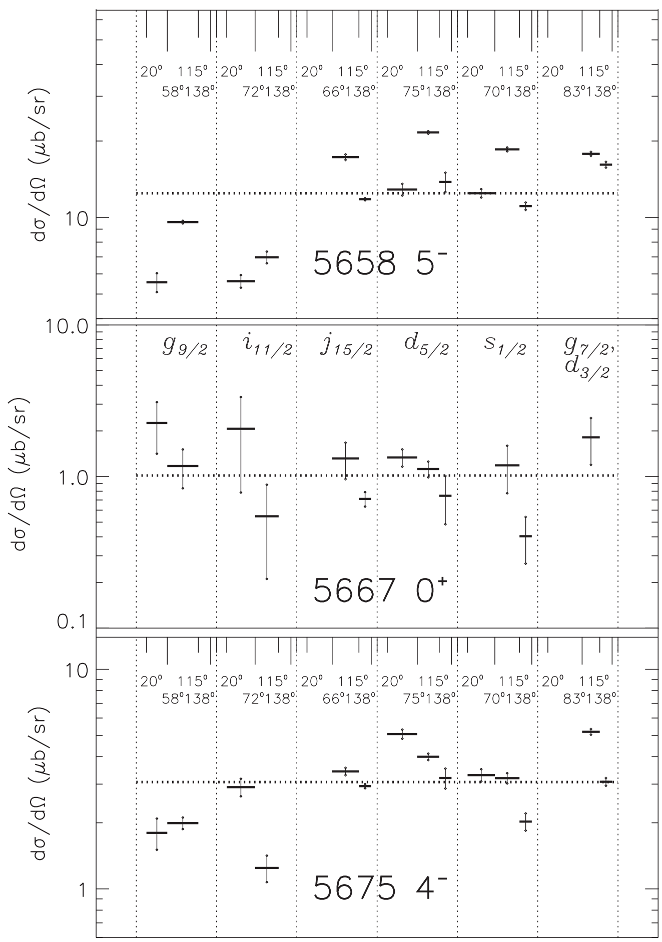

FIG. 2. For the 5658 5^-, 5667 0^+, and 5675 4^- states, angular distributions of cross sections at $20^\circ < \Theta < 138^\circ$ near seven IARs (Table II) or excitation functions from $E_p = 14.8$ to 17.6 MeV for four ranges of scattering angles shown in the first and third frame. For details see Sec. IV B 2.

E. The mixing among the four lowest 0^+ states

The 4868 state was identified as the neutron pairing vibration 0^+ state by Igo *et al.* [19]. The 5241 state was identified as the d.o. 0^+ state [17,18]. Yeh *et al.* [17] derived the spin of 0 from the angular distribution in the ^{208}Pb$(n,n'\gamma)$ reaction. Orce *et al.* [18] determined the branching ratio $E3(0_3^+ \to 3_1^+)/E0(0_3^+ \to 0_1^+)$ in agreement with predictions for a two-phonon octupole transition.

TABLE II. Range of proton bombarding energies E_p chosen to study the ^{208}Pb(p,p') reaction. $E_{LJ}^{\rm res}$ is the energy of the IAR, $\Gamma_{LJ}^{\rm tot}$ the width.

LJ	$E_p - E_{LJ}^{\rm res}$ MeV	$E_{LJ}^{\rm res}$ [8,38] MeV	$E_p - E_{LJ}^{\rm res}$ MeV	$\Gamma_{LJ}^{\rm tot}$ [8,38] MeV
$g_{9/2}$	−0.10	14.92	+0.15	0.25
$i_{11/2}$		15.72		0.22
$j_{15/2}$	−0.12	16.38		0.21
$d_{5/2}$	−0.06	16.45	+0.18	0.31
$s_{1/2}$		16.96		0.32
$g_{7/2}$	−0.25	17.43		0.29
$d_{3/2}$		17.48	+0.24	0.28
off-resonance	−0.10	18.00	+0.14	

The existence of the proton pairing vibration 0^+ state is without doubt since nuclear forces between neutrons and protons do not differ much [37]. The influence of the Coulomb force, however, is large; hence the excitation energy is predicted within a considerable uncertainty [Eq. (7)]. In Sec. IV B, the 5667 state is identified as the proton pairing vibration 0^+ state.

The four lowest 0^+ configurations in ^{208}Pb are the bare doubly magic ^{208}Pb core, the neutron and the proton pairing vibration and the d.o. configurations,

$$\begin{aligned} 0^+_{\rm g.s.} &\equiv {}^{208}\text{Pb(core)},\\ 0^+_{\nu} &\equiv {}^{206}\text{Pb(g.s.)} \otimes {}^{210}\text{Pb(g.s.)},\\ 0^+_{\pi} &\equiv {}^{206}\text{Hg(g.s.)} \otimes {}^{210}\text{Po(g.s.)}, \quad \text{and}\\ 0^+_{d.o.} &\equiv {}^{208}\text{Pb}(3_1^-) \otimes {}^{208}\text{Pb}(3_1^-). \end{aligned} \tag{12}$$

The four lowest 0^+ states, the yrast state 0_1^+, the 4868 0_2^+, 5241 0_3^+, and 5667 0_4^+ states essentially share the four lowest 0^+ configurations.

We assume the yrast 0^+ state to be rather pure,

$$0_1^+ = t_{11}0^+_{\rm g.s.} + t_{12}0^+_{\nu} + t_{13}0^+_{d.o.} + t_{14}0^+_{\pi},$$

with configuration strengths

$$|t_{11}|^2 \approx 1,\ |t_{12}|^2 \ll 1,\ |t_{13}|^2 \ll 1,\ |t_{14}|^2 \ll 1. \tag{13}$$

The excited 0^+ states are expected to be more mixed:

$$\begin{aligned} 0_2^+ &= t_{21}0^+_{\rm g.s.} + t_{22}0^+_{\nu} + t_{23}0^+_{d.o.} + t_{24}0^+_{\pi},\\ 0_3^+ &= t_{31}0^+_{\rm g.s.} + t_{32}0^+_{\nu} + t_{33}0^+_{d.o.} + t_{34}0^+_{\pi},\\ 0_4^+ &= t_{41}0^+_{\rm g.s.} + t_{42}0^+_{\nu} + t_{43}0^+_{d.o.} + t_{44}0^+_{\pi}. \end{aligned} \tag{14}$$

The admixtures of the bare core $0^+_{\rm g.s.}$ in the three lowest excited 0^+ states are expected to nearly vanish:

$$|t_{21}|^2 \ll 1, \quad |t_{31}|^2 \ll 1, \quad |t_{41}|^2 \ll 1. \tag{15}$$

Similarly because of the large distance from the three configurations 0^+_{ν}, $0^+_{d.o.}$, and 0^+_{π}, amplitudes of higher configurations are expected to be small. The next highest configuration explicitly mentioned by Curutchet *et al.* [22] is predicted as the coupling of two 5^- yrast states:

$$E_x(5_1^- \otimes 5_1^-) = 6396\ \text{keV}. \tag{16}$$

[The dominant configuration $g_{9/2}^{+2\nu}p_{1/2}^{-2\nu}$ is predicted at $2E_x^{SSM}(g_{9/2}p_{1/2}) = 6862$ keV.]

F. States excited by the ^{208}Pb(α,α') reaction

Excitation energies and cross sections for states excited by the ^{208}Pb(α,α') reaction at $E_x < 6.1$ MeV where determined by Atzrott [25] and Valnion *et al.* [27,28]; they are shown for $E_x > 4.6$ MeV in Table I. The resolution was about 11 keV and 8–10 keV, respectively.

Excitation strengths β_L are included both for the ^{208}Pb(α,α') and ^{208}Pb(p,p') reactions [1,25,34]; the strengths β_L of both reactions are similar for all resolved states. Yet the

TABLE III. Data for neighbors of the first three excited 0^+ states in ^{208}Pb (printed bold face). The 5667 state is identified as the proton pairing vibration state (Sec. IV B). The 4868 state was identified as the neutron pairing vibration state [19], the 5241 state as the d.o. 0^+ state [17,18]. Each state is given a unique energy label $\tilde{E}_x$. For $^{208}\mathrm{Pb}(p,p')$, the excitation energy and mean cross section in four regions of the bombarding energies E_p near IARs in ^{209}Bi are shown (Table II). The angular distribution for $^{208}\mathrm{Pb}(p,p')$ mostly varies with the IAR and the scattering angle by a large factor; the uncertainty in the cross section includes the variability.

$\tilde{E}_x$	I^π_m	E_x	This work				[25]		[27,28]		This work for $^{208}\mathrm{Pb}(p,p')$							
	[12]	[1]	$^{207}\mathrm{Pb}(d,p)$		$^{208}\mathrm{Pb}(d,d')$		$^{208}\mathrm{Pb}(\alpha,\alpha')$				*next two lines:* near E_p(MeV) and IAR(s) in ^{209}Bi							
	[a]	keV	E_d(MeV) 22, 24		E_d(MeV) 22, 24		E_α(MeV) 40.4		40.0		14.8–15.8 $g_{9/2}, i_{11/2}$		16.1–16.4 $j_{15/2}$		16.4–16.8 $d_{5/2}$		16.8–18.2 $s_{1/2}$ - $d_{3/2}$	
			1. line:			...			...		Excitation energy and uncertainty in keV							
			2. line:			...			...		Mean cross section and uncertainty in μb/sr							
4861	8^+_2	4860.78 ± 0.06	4860.9	0.1	4860.4	0.1	4864.4[b]	1.4	4856.0	3.0	4860.6	0.1	4860.8	0.1	4860.7	0.1	4860.6	0.1
			40	10	5	2			≈20		1.5	0.5	10	2	6	3	3	1
4867	7^+_1	4867.91 ± 0.04	4868.0	0.1	4867.8	0.2	[b]		4868.0[b]	3.0	4867.8	0.2	4867.8	0.1	4867.9	0.1	4867.8	0.1
			100	20	8	2			<20		2	1	30	10	15	5	3	2
4868	$\mathbf{0^+_2}$	4868.35 ± 0.05	[c]		4868.3	0.3	[b]		[b]		4868.3	0.2	[c]		4868.4	0.2	4868.5	0.2
					5	5					2	1			5	3	4	2
5239	4^-_8	5239.3 ± 0.4	[c]		5239.8	0.1	[b]		[c]		5239.5 [d]	0.2	5239.1	0.4	5239.4	0.1	5239.5	0.3
					8	3					15 [d]	5	2	1	2	1	2	1
5241	$\mathbf{0^+_3}$	5241.1 ± 0.3	[c]		5240.6	0.1	[b]		5243.0[b]	0.8	5241.0	0.2	5240.7	0.2	5241.2	0.3	5241.1	0.1
					8	2			25		4	2	1.5	0.4	2.0	1.0	1.5	1.0
5245	3^-_8	5245.246 ± 0.021	5245.0	0.3	5245.1	0.1	5245.2[b]	0.1	[b]		5245.2	0.1	5245.1	0.1	5245.3	0.1	5245.2	0.1
			800	200	20	5					8	4	60	20	120	20	10	3
5658	5^-_{12}	5658.51 ± 0.04	5658.6	0.2	5658.5	0.1	5661.5 [f]	1.2	5656.5	1.5	5658.5 [e]	0.1	5658.7	0.1	5650.5	0.1	5658.2	0.1
			8	2	15	3			25		10 [e]	3	15	5	20	5	15	5
5667	$\mathbf{0^+_4}$	5665.7 ± 1.1	[c]		5666.7	0.4	[f]		5665.0	1.5	5666.6	0.4	5666.9	0.3	5667.0	0.2	5666.7	0.7
					0.7	0.5			35		1.5	1.0	1.5	1.0	1.5	1.0	1.5	1.0
5675	4^-_{11}	5675.366 ± 0.023	5675.7	0.2	5675.4	0.4	[c]		[c]		5675.3	0.1	5675.5	0.1	5675.2	0.1	5675.1	0.1
			10	5	4	1					2	1	3	2	5	2	4	2
5686	6^-_8	5686.5 ± 0.7	[c]		5686.3	0.1	[c]		[c]		5686.1 [e]	0.1	5686.4	0.1	5686.1	0.1	5686.2	0.1
					8	3					15 [e]	5	3	2	3	2	4	2
5690	4^+_4	5690.117 ± 0.023	5690.0	0.2	5690.0	0.1	[c]		5690.8	0.8	5689.7	0.1	5689.9	0.1	5689.9	0.1	5689.8	0.1
			3	1	40	5			114		8	4	10	3	12	4	15	5
5694	7^-_5	5694.22 ± 0.12	[c]		5694.7	0.1	5694.2	1.2	[c]		5694.9 [e]	0.1	5695.0	0.1	5695.0	0.1	5694.8	0.1
					8	2					15 [e]	5	3	2	3	2	5	3

[a] The order number m is determined by [12].
[b] Not resolved.
[c] Not observed.
[d] Excitation energy and mean cross section on $i_{11/2}$ IAR.
[e] Excitation energy and mean cross section on $g_{9/2}$ IAR.
[f] See Sec. IV B 1.

TABLE IV. Excitation energies of levels near 5.66 MeV. The final results for the 5676 0^+ state are printed bold face.

N	E_x keV	Reaction	$\overline{d\sigma/d\Omega}$ μb/sr	Ref.
1	5658.8 ± 0.3	^{208}Pb(p,p')		[34]
2	5658.4 ± 1.5	^{207}Pb(d,p)		[27]
3	*5656.5* ± 1.5	^{208}Pb(α,α')	25	[27]
4	5655.3 ± 1.5	^{208}Pb(d,d')		[27]
5	5658.8 ± 2.5	^{208}Pb(p,p')	21	[27]
6	5658.51 ± 0.04			[1]
7	5658.6 ± 0.2	^{207}Pb(d,p)	8 ± 2	a
8	5658.5 ± 0.1	^{208}Pb(d,d')	15 ± 3	a
9	5658.6 ± 0.2	^{208}Pb(p,p')	10 - 20	b
10	5665.1 ± 0.3	^{208}Pb(p,p')	18 ± 2	[16]c
11	5661.5 ± 1.2	^{208}Pb(α,α')		[25]
12	*5661.5* ± 1.1	^{208}Pb(α,α')		d
13	5666.4 ± 1.5	^{208}Pb(p,p')	2	[27]
14	*5665.0* ± 1.5	^{208}Pb(α,α')	35	[27]
15	5665.7 ± 1.1			[1]
16	**5666.7 ± 1.0**	^{208}Pb(d,d')	0.7 ± 0.5	a
17	**5666.7 ± 0.3**	^{208}Pb(p,p')	1.0 ± 0.3	b

[a]This work, see Table III.
[b]This work, see Table III and Fig. 2.
[c]On $d_{5/2}$ IAR in ^{209}Bi.
[d]Mean value of the excitation energies shown at $N = 3,14$ weighted by the cross sections $\sigma(25^\circ)$ shown under $\overline{d\sigma/d\Omega}$.

^{208}Pb(p,p') reaction excites also unnatural parity states similar to the ^{208}Pb(d,d') reaction.

In the ^{208}Pb(α,α') spectrum shown by Valnion *et al.* [26] the 5667 state clearly shows up. The cross section at $\Theta = 25^\circ$ is 38 μb/sr (Table I), twice the upper limit observed by Valnion *et al.* [27,28]. In the experiment with lower resolution [25] the 5.6 MeV level is significantly shifted away from the 5658 5^- state (Sec. IV B 2). Few exceptions from the statement, that the ^{208}Pb(α,α') reaction excites only natural parity states, are apparent.

Solely, two levels have cross sections larger than the lower limit of about 20 μb/sr and are not recognized to correspond to a natural parity state, namely the 5042 and 5667 levels. [The level at $E_x = 5835$ keV is identified as the 5825 state with the spin of 8^+; the new spin assignment is based on the excitation in the ^{208}Pb(d,d') and ^{207}Pb(d,p) reactions, details are not discussed here. L satellites from the 5813 state may be present, too, see Sec. III C 1.]

The excitation of the 5.04 MeV level is explained by the presence of a doublet consisting of the 5038 2_2^- state [7] and a new state about 5 keV higher. The reanalysis of the Q3D data clearly reveals the 5042 state with a mean cross section of a few μb/sr.

The low excitation energy excludes the assignment as the proton pairing vibration state [Eq. (7)]. We suggest the 5042 state to have the spin of 2^+. Details of the identification are beyond the scope of this paper. The 5667 state is the single level stronger excited by the ^{208}Pb(α,α') reaction and not associated with a state of known spin [1,5–16].

III. EXPERIMENTS ON PARTICLE SPECTROSCOPY AT THE MLL

Since 2003, experiments on particle spectroscopy were performed with the Q3D magnetic spectrograph and the final detector [30] at the Maier-Leibnitz-Laboratorium (Garching, Germany) [5–15]. The resolution is 1.5 keV half-width at half-maximum on the low energy side [8] and 2-5 keV on the high energy side.

A. Studied reactions

We studied the ^{208}Pb(p,p') reaction with bombarding energies $14.8 < E_p < 18.2$ MeV at scattering angles from 20° to 138°. The proton energies E_p covered the isobaric analog resonances (IAR) in ^{209}Bi corresponding to the single particle orbits LJ and an off-resonance region (Table II).

About 300 levels with excitation energies in ^{208}Pb from 2.6 MeV to 8.0 MeV were observed, correspondingly the energies of the emitted particles were $E_{p'} = 7$–14 MeV. About 350 spectra were taken during around 250 h of actually used beam-time (run-time). A typical ^{208}Pb(p,p') spectrum covers 0.9 MeV in excitation energy.

We studied the ^{208}Pb(d,d') reaction with deuteron energy $E_d = 22$ MeV at scattering angles from 15° to 50° and $E_d = 24$ MeV at scattering angles from 30° to 112°. The energies of the emitted particles were $E_{d'} = 14$–19 MeV. About 50 spectra were taken during around 20 h of run-time.

We studied the ^{206,207,208}Pb(d,p) reactions with deuteron energy $E_d = 22$ MeV at scattering angles from 15° to 50° and $E_d = 24$ MeV at scattering angles from 30° to 112°. The energies of the emitted particles were $E_p = 11$–16 MeV. About 70 spectra were taken during around 40 h of run-time.

B. Experimental data

The main source of experimental data derives from the study of the resonant and nonresonant ^{208}Pb(p,p') reaction, but the study of the ^{208}Pb(d,d') and ^{207}Pb(d,p) reactions is also important. Inelastic proton scattering via isobaric analog resonances (IAR) is equivalent to a neutron pickup reaction on a target in an excited state. Hence, in effect ten different particle exchange reactions with final states in ^{208}Pb were studied.

While nuclear states in ^{208}Pb are excited by the ^{207}Pb(d,p) reaction and ^{208}Pb(p,p') via IAR in ^{209}Bi in a highly selective manner, the ^{208}Pb(d,d') reaction excites almost all states with little selectivity; the cross section is weakly correlated to the spin of the state and in a limited manner to the structure. The strength of the excitation is similar to the nonresonant (p,p') reaction and for natural parity to the ^{208}Pb(α,α') reaction (Table I).

The analysis of all data obtained with the Q3D magnetic spectrograph was performed using the computer code GASPAN [39]. Table III shows excitation energies and mean cross sections for neighbors of the first three excited 0^+ states. They are determined from experiments with the ^{208}Pb(α,α') reaction [25–28] and by this work for the ^{208}Pb(p,p') reaction with proton energies shown in Table II and by the ^{207}Pb(d,p), ^{208}Pb(d,d') reactions.

Figure 1 shows spectra constructed by summing up several spectra taken under different conditions but near one out of the seven known IARs. They are smoothed because of the quadratic dependence of the width of peaks in individual spectra on the position in the detector of the Q3D magnetic spectrograph. They are fitted by GASPAN [39] in the usual manner. The 5667 level is marked magenta.

The main arguments for the selection of spectra were (i) good resolution, (ii) low background, and (iii) similarity of the relative cross sections near the chosen bombarding energies. Hence, the relative cross sections do not have a meaning because of the arbitrary selection of scattering angles. The excitation energies are less precise than determined from single spectra because of the reduced resolution. Yet the tenfold increased statistics better reveal weak peaks.

The 5649 9^+ state is strongly excited near the $j_{15/2}$ IAR and still with about half the strength at the bombarding energy corresponding to the $d_{5/2}$ IAR and nearby. The 5643 2^- and 5648 3^- states are strongly excited near the $d_{5/2}$ IAR and still with about half the strength at the bombarding energy corresponding to the $j_{15/2}$ IAR and nearby (Table II).

On the $g_{9/2}$ IAR: Eight spectra taken were taken at scattering angles $58^\circ \leqslant \Theta \leqslant 112^\circ$ with four different targets. The total beam time used was about 150 minutes. The 5658 5^-, 5687 6^-, and 5694 7^- states are excited with mean cross sections of about 15 μb/sr [9]. The 5640 1^-, 5643 2^-, and 5690 4^+ states are not resolved; the 5649 9^+ state is not excited.

On the $i_{11/2}$ IAR: Twelve spectra taken were taken at scattering angles $25^\circ \leqslant \Theta \leqslant 115^\circ$ with the same target except for one run. The total beam time used was about 250 minutes. The 5640 1^- and 5643 2^- states are not resolved; the 5687 6^- and 5694 7^- states are weakly excited; the 5649 9^+ state is not excited.

Near the $j_{15/2}$,$d_{5/2}$ IARs: Eleven spectra were taken at scattering angles $42^\circ \leqslant \Theta \leqslant 48^\circ$ and 138° with five different targets. The bombarding energies were from $E_p = 16.390$ to $E_p = 16.500$ MeV. The total beam time used was about 250 minutes. The 5667 state is marginally identified because of the presence of the L satellites from the 5648 3^- and 5649 9^+ states; similar L-satellites from the 5643 2^- state are present (shown in blue).

Near the $g_{7/2}$,$d_{3/2}$ doublet IAR: With two different targets, eight spectra were taken at scattering angles $84^\circ \leqslant \Theta \leqslant 138^\circ$. The bombarding energies were from $E_p = 17.300$ to $E_p = 17.660$ MeV. The total beam time used was about 150 min. The flat background is lower by a factor of about 2 than for the summed spectra taken on the $g_{9/2}$, $i_{11/2}$, $j_{15/2}$, and $d_{5/2}$ IARs. The 5640 1^- and 5643 2^- states are resolved; the 5687 6^- and 5694 7^- states are weakly excited; the 5649 9^+ state is not excited.

The ^{208}Pb(d,d') reaction: With two different targets, 16 spectra were taken at scattering angles $32^\circ \leqslant \Theta \leqslant 44^\circ$ and the bombarding energy $E_d = 22$ MeV. The total beam time used was about 800 min. All states are resolved except for the 5648 3^-_{13}, 5649 9^+_4 doublet with a distance 0.5 keV [8]; here, a larger width was used to fit the level by GASPAN.

C. Peak shape in spectra taken with the Q3D magnetic spectrograph

In particle scattering experiments [here ^{208}Pb(p,p'), ^{208}Pb(d,d'), and ^{207}Pb(d,p)], the peak shape is highly asymmetric for two major reasons, (i) the knockout of atomic electrons, (ii) the energy loss from the passage of the escaping particle through the atomic layers of the target.

The former effect results in a structured tail with many satellites (Sec. III C 1) while the latter effect generates a smooth tail because of the stochastic straggling in the atomic layers of the target. By proper mounting of the target, the crossing of the escaping particle through the carbon backing can be avoided at backward scattering angles.

1. Satellites from the knockout of atomic electrons

In the ^{208}Pb(p,p') reaction via the seven known IARs in ^{209}Bi (Table II) protons have a typical energy of 10 MeV. The instrumental resolution of the Q3D magnetic spectrograph is about 2.5 keV for such protons. Many of the 82 atomic electrons in lead have binding energies larger than the instrumental resolution, especially the innermost electrons have binding energies

$$\begin{aligned} E_B(e) = 88.005 &\quad \text{keV for } K\text{–electrons}, \\ 13.055, 15.200, 15.861 &\quad \text{keV for } L_{I,II,III}\text{–electrons}, \\ 2.484 - 3.851 &\quad \text{keV for } M_{I,\ldots,V}\text{–electrons}. \end{aligned} \tag{17}$$

The inelastic scattered proton escaping from the nucleus looses energy from the simultaneous knockout of up to 82 electrons. The 18 M-electrons limit the resolution to about 3 keV. The 54 N-, O-, P-electrons produce a structured, unresolved tail to each peak.

For each main peak from a particle reaction like ^{208}Pb(p,p'), ^{208}Pb(d,d'), or ^{207}Pb(d,p), there are 23 resolved satellites in a distance of

$$\begin{aligned} \Delta E^{\text{sat}} &\approx k \cdot 88 + l \cdot 15 \text{ keV}, \\ k &= 0,1,2 \text{ and } l = 0,\ldots,8. \end{aligned} \tag{18}$$

K satellites without L electrons ($l = 0$) cannot be distinguished from another main peak by its peak shape; only the strict correlation of the intensity to the main peak announces the satellite.

The L-satellites are broader than the main peak because of the spread of the binding energies; the width increases with the number of emitted L electrons by about $2.5 \cdot l$ keV [Eqs. (17), (18)]. A fit by GASPAN is able to distinguish an L satellite from another main peak if the width of the peak can be determined with sufficient precision.

The probability to produce a satellite depends on the scattering angle and the energy of the escaping proton. K-satellites have a cross section of less than one permille of the main peak; they are observed only in spectra with a peak-to-valley ratio larger than a few thousand. We have several such spectra where up to a dozen satellites are observed for a single physical state in lead. The highest peak-to-valley ratio observed was 10 000.

L satellites from the knockout of one L electron have a cross section of about 1% of the main peak, those with two L electrons about half of the cross section for the first L satellite and so on; they are annoying in the analysis of spectra taken with Q3D magnetic spectrograph. (In earlier spectra taken before 2003 the knockout of atomic electrons was not considered because the resolution was worse. In some instances it is well visible, even in spectra taken in 1968-1969 with a resolution of 12 keV [16] because of the large peak-to-valley ratio.)

The computer code GASPAN evaluates the width of each peak with a precision of eV. As the Q3D magnetic spectrograph registers the momentum of the proton, the width varies by a factor of about 2 across the whole length of the detector. We use the last digit set to 0 in order to tag each peak whether it is due to an inelastically scattered proton from the ^{208}Pb(p,p') reaction [and correspondingly from the ^{207}Pb(d,p) and ^{208}Pb(d,d') reactions] without the emission of a K or L electron. A last digit set to 1–9 indicates either a K or L satellite or a peak on a high background (mostly broad peaks from the reaction on ^{1}H, ^{2}H, ^{12}C, ^{14}N, ^{16}O, or ^{40}Ar). In the subsequent analysis with other evaluation tools, only the peaks with the last digit set to 0 in the width are considered as physical levels in lead.

For each main peak only few satellites are really observed above the smooth background [13]. A typical peak-to-valley ratio is 100, but often less. Mostly, only the first L satellite at about 15 keV distance from the main peak is discerned. GASPAN can fit a main peak close to an L satellite, but the order of the two peaks is often arbitrary; here some human guidance is needed.

2. Satellites near the 5667 state

Near the 5667 state, K satellites accompanied by L satellites [Eq. (18)] arise from the strong excitation of the 5564 3^- state with the emission of one K electron and of the 5482 5^-, 5512 1^-, 5517 3^- states with two K electrons. Yet, the relative intensities are below the general background in all cases. K satellites contribute less than 10% to the observed intensity of the 5667 level, but they may change the position slightly (Sec. III C 3).

Near the 5667 state, L satellites arise from the excitation of the 5643 2^-, 5648 3^-, 5649 9^+, and 5658 5^- states. Near the $j_{15/2}$ and $d_{5/2}$ IARs at scattering angles $\Theta \lesssim 50^\circ$ and $\Theta = 138^\circ$ the angular distribution of the 5643 2^- state raises up. It has a minimum at $\Theta = 90^\circ$ indicating a purely resonant reaction. Also the 5648 3^- and 5649 9^+ states have large cross sections. Hence, L satellites show up near $E_x \approx 5643 + 15$ and $5648 + 15$ keV. Indeed in the fit by GASPAN of the summed spectrum shown in Fig. 1, the two L satellites show up (marked blue). Hence, the position of the 5667 state can be determined with difficulty only near the $j_{15/2}$ and $d_{5/2}$ IARs.

Luckily the 5643 2^-, 5648 3^-, and 5649 9^+ states have low cross sections on the $g_{9/2}$ and $i_{11/2}$ IARs. The 5667 state is clearly distinguished from the background generated by the long tail from the 5658 5^- state and the flat background from stray particles. Near the $g_{7/2}$ and $d_{3/2}$ IARs, the general background is twice lower and hence the 5667 state is observed even more clearly; the weak 5640 1^- state with a mean cross section of about 0.3 μb/sr is well recognized.

3. Systematic uncertainties caused by the peak shape

The large asymmetry of each peak derives from the sum of satellites of M,N,O,P electrons and the scattering of the escaping proton within the target. GASPAN fits the tail with an exponential function [8]. Yet the width of the Gaussian and the length of the tail are correlated. The width of the Gaussian is arbitrarily fixed to some linear function on the position in the detector where the parameters are once determined for some well isolated peaks in spectra taken under similar conditions. The width of the exponential tail varies inversely with the Gaussian width. As a consequence, the position of a weak peak sitting on the tail of a strong peak varies slightly with the choice of the fit parameters.

In case the 5648 3^- and 5649 9^+ states are more than ten times stronger excited than the 5667 state, L satellites are significant. In many cases the order of the two L satellites is arbitrary or they cannot be distinguished from the physical peak of the 5667 state. A systematic uncertainty of around 0.3 keV in the excitation energy is then estimated for the weak peak of the 5667 state.

IV. DISCUSSION

A. Identification of the states at $E_x = 4686$, 5241, and 5667

1. The 4868 state

We confirm the excitation energies of the 0.5 keV doublet consisting of the 4867 7_1^+ and 4868 0_2^+ states with a precision of 200 eV (Table III). While the 4867 7_1^+ is strongly excited in the ^{208}Pb(p,p') reaction on the $j_{15/2}$ IAR and in the ^{207}Pb(d,p) reaction, the 4868 0_2^+ state shows up in the ^{208}Pb(p,p') reaction at proton energies far off the $j_{15/2}$ IAR and in the ^{208}Pb(d,d') reaction. Smooth excitation functions with cross sections of about 3 μb/sr are observed (Table III).

2. The 5241 state

We confirm the excitation energies of the 5 keV doublet consisting of the 5239 4_8^- [5], 5241 0_3^+, and 5245 3_8^- states with a precision of 200 eV (Table III). While the 5239 4_8^- state is excited on the $i_{11/2}$ and $g_{7/2}$ IARs, and the 5245 3_8^- state on the $d_{5/2}$ IAR and by the ^{207}Pb(d,p) and ^{208}Pb(d,d') reactions, the 5241 0_3^+ state is clearly observed in the ^{208}Pb(d,d') reaction (Fig. 2 [15]) and in the ^{208}Pb(p,p') reaction outside the $i_{11/2}$, $d_{5/2}$ and $g_{7/2}$ IARs.

3. The 5667 state

In the region of $5.63 < E_x < 5.70$ MeV the cross section for seven states (5640 1_4^-, 5643 2_5^-, 5648 3_{13}^-, 5649 9_4^+, 5658 5_{12}^-, 5686 6_8^-, 5694 7_5^-) varies largely with the bombarding energy E_p in the ^{208}Pb(p,p') reaction whereas it does not change much for the 5675 4_{11}^- [12], 5690 4^+ [1,9] states, and especially for the 5667 state. Indeed, the 5640 1_4^-, 5686 6_8^-, 5694 7_5^- states are ten times stronger excited on the $g_{9/2}$ IAR than elsewhere [9], the 5649 9_4^+ ten times stronger on the $j_{15/2}$ IAR [8], the 5643 2_5^- state even 50 times stronger on the $d_{5/2}$ IAR [12].

Similarly, the 5648 3_{13}^- and 5658 5_{12}^- states are selectively excited both on the $g_{9/2}$ and $d_{5/2}$ IARs [8,9]. The 5675 4_{11}^- state has a dominant $h_{9/2}d_{5/2}$ component and only minor admixtures of neutron particle-hole configurations [12].

The 5667 state is observed in about two dozen out of more than 100 spectra, especially near the $g_{9/2}$ and $i_{11/2}$ IARs where L satellites from the 5643 2_5^-, 5648 3_{13}^-, 5649 9_4^+ are negligible. Hence, the excitation energy can be determined rather precisely (Tables III, IV).

In Fig. 1, the 5667 0_4^+ state is excited with a similar cross section as the 5675 4_{11}^- state. In spectra for ^{208}Pb(p,p') taken on the $g_{9/2}$ IAR at $\Theta = 25°,42°,58°$ shown in Fig. 3 [9] and Fig. 1 [14] with different fits by GASPAN the peak at 5667 keV is not fitted; it is similarly strong as the well-recognized peaks at $E_x = 5640$ and 5643 keV. In a spectrum for ^{207}Pb(d,p) taken in the region $5.59 < E_x < 5.70$ MeV (Fig. 3 [15]), the peak at 5665 keV derives from a contamination by a light nucleus (probably ^{40}Ar).

B. Identification and structure of the proton pairing vibration state

1. Excitation energy of the proton pairing vibration state

The proton pairing vibration state is located at $E_x =$ 5667 keV. The clear excitation by the ^{208}Pb(α,α') reaction [25,26] indicates natural parity. The excitation energies of the 5658 5^- and 5667 states and their cross section $\sigma(25°)$ at the scattering angle of $\Theta = 25°$ were determined by Valnion *et al.* [27] (Tables III, IV).

Remarkably, the ^{208}Pb(α,α') experiment performed by Atzrott [25] yields an excitation energy corresponding to the mean energy calculated from the results obtained by Valnion *et al.* [27], see under $N = 3,12$, and 14 in Table IV (in italic). The angular distribution of the 5661.5 keV level is much steeper than for the 3708 5^- state, especially for $50° < \Theta < 90°$ [25].

2. Angular distribution of the 5667 state

Figure 2 shows cross sections of the 5658 5^-, 5667, and 5675 4^- states determined near each of the seven IARs (Table II). The scale is logarithmic. The global mean value is shown by the long dotted line. Near each IAR the mean cross section is determined for scattering angles $20° \leqslant \Theta \leqslant 138°$. Three different ranges of scattering angles were chosen on each IAR.

The angular distribution of the 5658 5^- state is well described by a series of even-order Legendre polynomials up to sixth degree [9]; it varies by a factor of three from one scattering angle to another, even within the range $60° \leqslant \Theta \leqslant 90°$. The angular distribution of the 5675 4^- state reveals a considerable contribution from the nonresonant ^{208}Pb(p,p') reaction by the raise towards forward angles. The angular distribution of the 5667 0^+ state is smooth with some raise towards forward angles, too. The mean cross section is

$$\overline{\delta\sigma/\delta\Omega}\,(5667) = 1.0 \pm 0.3\ \mu\text{b/sr}. \tag{19}$$

3. Determination of spin and parity

Below $E_x = 5.86$ MeV all negative parity states predicted by the SSM are identified [12], hence the parity of the 5667 state is positive. The excitation function is smooth with a mean cross section of about 1 μb/sr [Eq. (19), dotted line in Fig. 2.] The angular distributions raising towards forward angles and the smoothness of the excitation functions indicate a nonresonant reaction. The congruence of the excitation energy with the expected energy of the 0_π^+ state [Eq. (7)] yields the assignment of spin 0^+ to the 5667 state.

The spin of 2^+ and higher spins are ruled out. Namely, the number of states with spins 2^+, 4^+, 6^+, 8^+, 10^+ agrees with the number of states expected from the SSM and as members of the d.o. configuration. Similar to the 1^- and 3^- yrast states appearing in addition to the predictions by the SSM [12], the 2^+ yrast state is assumed to appear in addition, too. There are doubts about the existence of some levels which can be ruled out by the renewed analysis of the existing Q3D data; details are beyond the scope of this paper.

In the ^{206}Pb(p,t) reaction [20], the ratio of the cross sections for the 4868 and 5241 states is about 10:1. In the ^{210}Pb(t,p) reaction no comparison could be done since the 5245 3^- state is stronger excited. The 5667 state is not detected in the ^{206}Pb(p,t) and ^{210}Pb(t,p) reactions; no level between the 5640 1_4^- and 5690 4^+ states (level 48 and 50 [20]) is reported.

By identifying the 5667 state as the proton pairing vibration state and by assuming a pure 0_π^+ configuration [Eq. (14) with $t_{44} \approx 1$], the Coulomb displacement energy is derived from Eq. (6) as

$$\delta E^\pi_{\text{Coul}}(\text{ph}) = -233 \pm 20\ \text{keV}. \tag{20}$$

The uncertainty derives from the mass measurements [32]. An incomplete 0_π^+ strength in the 5667 0^+ state will change the value. Curutchet *et al.* [22] calculate a 20% admixture of higher configurations and hence a lower value $\delta E^\pi_{\text{Coul}}(\text{ph}) =$ -0.21 MeV.

4. Configuration mixing among the three lowest excited 0^+ *states*

Curutchet *et al.* [22] used the multistep shell-model method described by Liotta and Pomar [40] to calculate the configuration mixing among the 0^+ states in ^{208}Pb in dependence of the Coulomb displacement energy. The composition of the three first excited 0^+ states in terms of the neutron and pairing vibration and the d.o. configurations [Eq. (14)] is shown in their Fig. 1.

The configuration basis comprised more configurations besides 0_ν^+, $0_{d.o.}^+$, and 0_π^+. From Fig. 1(b) [22], however, the contribution of higher configurations in the 0_2^+, 0_3^+, and 0_4^+ states is determined to be less than 20%.

The energies of the states are

$$\begin{aligned} E_{22} &\equiv E_x(0_2^+) = 4868\ \text{keV},\\ E_{33} &\equiv E_x(0_3^+) = 5241\ \text{keV},\\ E_{44} &\equiv E_x(0_4^+) = 5667\ \text{keV}, \end{aligned} \tag{21}$$

see Secs. IV A, IV B.

The energies of the configurations are

$$\begin{aligned} e_{22} &\equiv E_x(0_\nu^+) = 4980\ \text{keV},\\ e_{33} &\equiv E_x(0_{d.o.}^+) = 5229\ \text{keV},\\ e_{44} &\equiv E_x(0_\pi^+) = 5650\ \text{keV}, \end{aligned} \tag{22}$$

see Eqs. (4), (5), (6) together with Eqs. (8), (9). Here we use the mean value from Eq. (7) for e_{44}.

In Fig. 1(a) [22] the excitation energy $E_x = 5667$ keV for the 0_4^+ state yields the value δE. Going to Fig. 1(b) [22] the strengths are determined as

$$\begin{aligned} t_{22}^2 &\approx (0.65 \pm 0.03)/1.00 \quad \text{for } E_x = 4868 \text{ keV}, \\ t_{33}^2 &\approx (0.55 \pm 0.03)/0.95 \quad \text{for } E_x = 5241 \text{ keV}, \\ t_{44}^2 &\approx (0.75 \pm 0.02)/0.80 \quad \text{for } E_x = 5667 \text{ keV}; \end{aligned} \tag{23}$$

the graphic presentation limits the precision. We neglect contributions from the higher configurations by the renormalizing factors 1.00,0.95,0.80.

By constructing an orthogonal matrix in a unique manner, we obtain the mixing amplitudes in the transformation from the space of configurations to the space of states [Eq. (14)],

$$\begin{pmatrix} t_{22} & t_{23} & t_{24} \\ t_{32} & t_{33} & t_{34} \\ t_{42} & t_{43} & t_{44} \end{pmatrix} = \begin{pmatrix} +0.80 & -0.58 & +0.13 \\ +0.59 & +0.75 & -0.29 \\ +0.07 & +0.31 & +0.95 \end{pmatrix}. \tag{24}$$

Evidently, the fourth 0^+ state is described as the rather pure proton pairing vibration configuration 0_π^+ while the neutron pairing vibration and the d.o. configurations are mixed with a ratio of about 2 : 1.

From the transformation matrix Eq. (24) together with the energies of the states [Eq. (21)] and the configurations [Eq. (22)], the matrix elements of the residual interaction can be calculated using the formalism described by [41].

The matrix elements of the residual interaction are calculated (Eq. (17a) [41]) as

$$v_{kl} = v_{lk} = \sum_n t_{kn} t_{ln} (E_{nn} - (e_{kk} + e_{ll})/2). \tag{25}$$

The diagonal values yield

$$\begin{aligned} v_{22} &= \langle 0_\nu^+ | \mathbf{v} | 0_\nu^+ \rangle = +30 \pm 20 \text{ keV}, \\ v_{33} &= \langle 0_{d.o.}^+ | \mathbf{v} | 0_{d.o.}^+ \rangle = -80 \pm 30 \text{ keV}, \\ v_{44} &= \langle 0_\pi^+ | \mathbf{v} | 0_\pi^+ \rangle = -30 \pm 20 \text{ keV}. \end{aligned} \tag{26}$$

The off-diagonal values are sensitive to the weak off-diagonal amplitudes but only weakly depend on the model energies. From Eqs. (21)–(24) we obtain

$$\begin{aligned} v_{23} = v_{32} &= \langle 0_\nu^+ | \mathbf{v} | 0_{d.o.}^+ \rangle = -180 \pm 30 \text{ keV}, \\ v_{24} = v_{42} &= \langle 0_\nu^+ | \mathbf{v} | 0_\pi^+ \rangle = +30 \pm 60 \text{ keV}, \\ v_{34} = v_{43} &= \langle 0_\pi^+ | \mathbf{v} | 0_{d.o.}^+ \rangle = -140 \pm 30 \text{ keV}. \end{aligned} \tag{27}$$

The uncertainty of the matrix elements of the residual interaction derives from the imprecise determination of the amplitudes [Eq. (23)].

The matrix elements between the neutron and the proton pairing vibration and the d.o. configuration are almost the same while all other matrix elements are vanishingly small. The symmetry of the residual interaction supports the assumption of protons and neutrons as nucleons interacting with nearly identic nuclear forces [37] while only the protons are affected by the additional electromagnetic force.

V. SUMMARY

By particle spectroscopy with the Q3D magnetic spectrograph at the MLL, the excitation energies of the neutron pairing vibration and d.o. 0^+ states are verified within 200 eV. The ^{208}Pb(p,p') reaction is shown to be nonresonant for $14.8 < E_p < 18.2$ MeV wherein seven IARs in ^{209}Bi are known. The cross sections at scattering angles from 20° to 138° are around 3 μb/sr. A new state is identified at 5042 ± 3 keV and suggested to have the spin of 2^+.

The proton pairing vibration state is identified at $E_x = 5666.7 \pm 0.3$ keV by the nonresonant ^{208}Pb(p,p') reaction and by the ^{208}Pb(d,d') reaction, both with cross sections of about 1 μb/sr. The identification is based on fact that the ^{208}Pb(α,α') reaction excites only states with natural parity which is proven for more than 40 other states and, in addition, the knowledge of five Coulomb displacement energies, two of them from unobservable particle-hole configurations [12].

By comparison to calculations using the multistep shell-model method [40] Curutchet *et al.* [22] show the 5667 state to contain the major strength of the proton pairing vibration configuration while the first and second excited 0^+ states contain the strongly mixed neutron pairing vibration and double octupole configurations.

The residual interaction between the neutron and proton pairing vibration configurations is deduced to be weak while the residual interaction between the pairing vibration 0^+ configurations and the double octupole 0^+ configuration is deduced to not depend on the isospin of the nucleon [37]. Protons and neutrons interact among the three lowest excited 0^+ states in the doubly magic nucleus ^{208}Pb by almost identic forces; electromagnetic forces contribute little.

ACKNOWLEDGMENTS

We thank P. E. Garrett, G. Graw, H.-L. Harney, J. Jolie, R. V. Jolos, R. Krücken, K.-H. Maier, and F. Riess for discussions.

[1] M. J. Martin, Nucl. Data Sheets **108**, 1583 (2007).
[2] J. H. D. Jensen and M. Goeppert-Mayer, *Elementary Theory of Nuclear Shell Structure* (Wiley, New York, 1955).
[3] L. W. Nordheim, Phys. Rev. **78**, 294 (1950).
[4] I. Talmi, *Contemporary Concepts in Physics*, Vol. 7, Simple Models of Complex Nuclei (Harwood Academic Publishers, Chur, Switzerland, 1993).
[5] A. Heusler, G. Graw, R. Hertenberger, F. Riess, H.-F. Wirth, T. Faestermann, R. Krücken, J. Jolie, D. Mücher, N. Pietralla, and P. von Brentano, Phys. Rev. C **74**, 034303 (2006).
[6] A. Heusler, G. Graw, R. Hertenberger, R. Krücken, F. Riess, H.-F. Wirth, and P. von Brentano, Phys. Rev. C **75**, 024312 (2007).
[7] A. Heusler, T. Faestermann, R. Hertenberger, R. Krücken, H.-F. Wirth, and P. von Brentano, Eur. Phys. J. A **46**, 17 (2010).

[8] A. Heusler, G. Graw, R. Hertenberger, F. Riess, H.-F. Wirth, T. Faestermann, R. Krücken, Th. Behrens, V. Bildstein, K. Eppinger, C. Herlitzius, O. Lepyoshkina, M. Mahgoub, A. Parikh, S. Schwertel, K. Wimmer, N. Pietralla, V. Werner, J. Jolie, D. Mücher, C. Scholl, and P. von Brentano, Phys. Rev. C **82**, 014316 (2010).
[9] A. Heusler, G. Graw, T. Faestermann, R. Hertenberger, H.-F. Wirth, R. Krücken, C. Scholl, and P. von Brentano, Eur. Phys. J. A **44**, 233 (2010).
[10] A. Heusler, T. Faestermann, R. Hertenberger, R. Krücken, H.-F. Wirth, and P. von Brentano, J. Phys. G (London) **38**, 105102 (2011).
[11] A. Heusler, R. V. Jolos, and P. von Brentano, Phys. At. Nucl. **76**, 807 (2013) [Yad. Fiz. **76**, 860 (2013)].
[12] A. Heusler, T. Faestermann, R. Hertenberger, H.-F. Wirth, and P. von Brentano, Phys. Rev. C **89**, 024322 (2014).
[13] A. Heusler, J. Phys.: Conf. Ser. **267**, 012038 (2011).
[14] A. Heusler, T. Faestermann, R. Hertenberger, H.-F. Wirth, and P. von Brentano, EPJ Web Conf. **66**, 02049 (2014).
[15] A. Heusler, J. Phys.: Conf. Ser. **580**, 012021 (2015).
[16] A. Heusler, H.-J. Glöckner, E. Grosse, C. F. Moore, J. Solf, and P. von Brentano, Eur. Phys. J. A **50**, 92 (2014).
[17] M. Yeh, P. E. Garrett, C. A. McGrath, S. W. Yates, and T. Belgya, Phys. Rev. Lett. **76**, 1208 (1996).
[18] J. N. Orce, T. Kibédi, G. D. Dracoulis, R. Julin, and S. W. Yates, J. Phys. G (London) **31**, S1705 (2005).
[19] G. J. Igo, P. D. Barnes, and E. R. Flynn, Phys. Rev. Lett. **24**, 470 (1970).
[20] G. Igo, P. D. Barnes, and E. R. Flynn, Ann. Phys. (NY) **66**, 60 (1971).
[21] J. Blomqvist, Phys. Lett. B **33**, 541 (1970).
[22] P. Curutchet, J. Blomqvist, R. J. Liotta, G. G. Dussel, C. Pomar, and S. L. Reich, Phys. Lett. B **208**, 331 (1988).
[23] P. Schuck, Z. Phys. A **279**, 31 (1976).
[24] B. A. Brown, Phys. Rev. Lett. **85**, 5300 (2000).
[25] U. Atzrott, Ph.D. thesis, Universität Tübingen, 1995.
[26] B. D. Valnion, W. Oelmaier, D. Hofer, E. Zanotti-Müller, G. Graw, U. Atzrott, F. Hoyler, and G. Staudt, Z. Phys. A **350**, 11 (1994).
[27] B. D. Valnion, Ph.D. thesis, Universität München, Herbert Utz Verlag, München, 1998.
[28] B. D. Valnion, V. Yu. Ponomarev, Y. Eisermann, A. Gollwitzer, R. Hertenberger, A. Metz, P. Schiemenz, and G. Graw, Phys. Rev. C **63**, 024318 (2001).
[29] M. Löffler, H. J. Scheerer, and H. Vonach, Nucl. Instrum. Methods Phys. Res. B **111**, 1 (1973).
[30] H.-F. Wirth, Ph.D. thesis, Technische Universität München, (2001), http://tumb1.biblio.tu-muenchen.de/publ/diss/ph/2001/wirth.html.
[31] J. P. Schiffer, Ann. Phys. (NY) **66**, 798 (1971).
[32] G. Audi, A. H. Wapstra, and C. Thibault, Nucl. Phys. A **729**, 337 (2003).
[33] J. H. Bjerregaard, Ole Hansen, O. Nathan, and S. Hinds, Nucl. Phys. **89**, 337 (1966).
[34] W. T. Wagner, G. M. Crawley, G. R. Hammerstein, and H. McManus, Phys. Rev. C **12**, 757 (1975).
[35] W. W. Daehnick, Phys. Reports **96**, 317 (1983).
[36] A. Bohr and B. R. Mottelson, *Nuclear Structure*, Vol. I (W. A. Benjamin, New York, 1969).
[37] W. Heisenberg, Z. Physik **77**, 1 (1932).
[38] W. R. Wharton, P. von Brentano, W. K. Dawson, and P. Richard, Phys. Rev. **176**, 1424 (1968).
[39] F. Riess, http://www.it.physik.uni-muenchen.de/dienste/software/gaspan/index.html Gamma-ray And particle SPectra interactive and automatic ANalysis (GASPAN) (2006).
[40] R. J. Liotta and C. Pomar, Nucl. Phys. A **362**, 137 (1981).
[41] A. Heusler and P. von Brentano, Ann. Phys. (NY) **75**, 381 (1973).